



# The treatment of petrochemical wastewater via ozone-persulfate coupled catalytic oxidation: mechanism of removal of soluble organic matter

Wenjing Guo<sup>1</sup> · Chong Li<sup>1</sup> · Janguang Zhao<sup>1</sup> · Yun Ding<sup>1</sup> · Qing Yang<sup>1,3</sup> · Hongxun Guan<sup>2</sup>

Received: 6 December 2023 / Accepted: 15 March 2024 / Published online: 4 April 2024  
© The Author(s), under exclusive licence to Springer-Verlag GmbH Germany, part of Springer Nature 2024

## Abstract

Petrochemical wastewater contains a variety of organic pollutants. Advanced oxidation processes (AOPs) are used for deep petrochemical wastewater treatment with distinct advantages, including the complete mineralization of organic substances, minimal residual byproducts, and compatibility with biological treatment systems. This work evaluates the effectiveness of three methods, namely, ozone, persulfate, and O<sub>3</sub>-PMS (ozone-persulfate) processes, which were compared to remove soluble organic matter. The O<sub>3</sub>-PMS process offered significant advantages in terms of organic matter removal efficiency. This process involves ozone dissolution in an aqueous persulfate solution, producing a more significant amount of hydroxyl radicals in comparison to single AOPs. The production of hydroxyl radicals and the synergistic effect of hydroxyl radicals and persulfate radicals were investigated. In the O<sub>3</sub>-PMS process, transition metal ions were added to understand the mechanism of the O<sub>3</sub>-PMS coupled catalytic oxidation system. The results showed that when the ozone concentration was in the range of 5 ~ 25 mg/L, the dosage of persulfate was in the range of 0.01 ~ 0.05 mol/L, the dosage of metal compounds was in the range of 0:0 ~ 2:1, and the reaction time was in the range of 0 ~ 2 h; the optimum chemical oxygen demand (COD<sub>Cr</sub>) and total organic content (TOC) removal effect was achieved under the coupled system with an ozone concentration of 10 mg/L, a persulfate dosage of 0.02 mol/L, a 1:2 dosage ratio of between Fe<sup>2+</sup> and Cu<sup>2+</sup> compounds, and a reaction time of 2 h. Under optimal reaction conditions, the rates of COD<sub>Cr</sub> and TOC removal reached 70% and 79.3%, respectively. Furthermore, the removal kinetics of the O<sub>3</sub>-PMS coupled catalytic oxidation system was analyzed to optimize the removal conditions of COD and TOC, and the mechanism regulating the degradation of dissolved organic matter was explored by three-dimensional fluorescence and GC-MS technology. Thus, O<sub>3</sub>-PMS coupled catalytic oxidation is an effective process for the deep treatment of wastewater. The careful selection of transition metal ions serves as a theoretical foundation for the subsequent preparation of catalysts for the ozone persulfate oxidation system, and this study provides a suitable reference for removing organic matter from petrochemical wastewater.

**Keywords** Petrochemical wastewater · AOPs · O<sub>3</sub>-PMS coupled catalytic oxidation

Responsible Editor: Guilherme Luiz Dotto

✉ Qing Yang  
369872832@qq.com

Wenjing Guo  
11210081@stu.lzjtu.edu.cn

Chong Li  
12211099@stu.lzjtu.edu.cn

Janguang Zhao  
0119011@stu.lzjtu.edu.cn

Yun Ding  
dingyun@mail.lzjtu.cn

Hongxun Guan  
guan hongxun@163.com

<sup>1</sup> School of Environmental and Municipal Engineering, Lanzhou Jiaotong University, Lanzhou 730070, China

<sup>2</sup> Beijing Tianhao Kerun Environmental Technology Co, Beijing 100176, China

<sup>3</sup> Engineering Research Center for Comprehensive Utilization of Water Resources in Cold and Drought Areas, Ministry of Education, Lanzhou Jiaotong University, Lanzhou, China

## Introduction

The petrochemical industry plays an essential role in the economic development of a country. Many important industries, such as energy, agriculture, and transportation, rely heavily on the petrochemical industry (Tian et al. 2020). However, petrochemical plants consume large quantities of water and subsequently generate wastewater (Wang et al. 2014). Petrochemical wastewater is characterized by high pollutant load, low biodegradability, high salinity, and toxicity (Kumar et al. 2013). Petrochemical wastewater comprises both organic pollutants like phenols, aldehydes, and benzenes, as well as inorganic pollutants such as heavy metals and fluoride. Given the severe health risks associated with these highly toxic pollutants (Gopalakrishnan and Bharathiraja. 2022), petrochemical wastewater must be treated before being safely released into the environment.

Based on the size of the pollutant particles, the PCW (petrochemical wastewater) pollutants are categorized into suspended, colloidal, and dissolved fractions. Although the suspended and colloidal traces can be simply removed by physicochemical treatment (Tong et al. 2016), the dissolved organic matter (DOM) contains many difficult-to-degrade compounds, such as benzene, aldehydes, phenols, polycyclic aromatic hydrocarbons (PAHs), naphthenic acids, petroleum hydrocarbons, and N/O/S-containing compounds. Such compounds require advanced and complex treatment strategies (Liu et al. 2014; Wang et al. 2021; Hayati et al. 2018).

Traditional methods for treating petrochemical wastewater involve adsorption or coagulation coupled with biological processes. However, these methods have limitations associated with process conditions. Hence, there is a growing need for alternative treatment approaches. Advanced oxidation processes (AOPs) emerge as a promising solution in this context. Various physical, chemical, and biological methods can treat petrochemical wastewater (Gopalakrishnan and Bharathiraja 2022). AOPs offer advantages such as the complete mineralization of organic matter, minimal residual material, and compatibility with biological systems (Fernandes et al. 2019, 2020). Among the various methods, the ozone-persulfate process is economically feasible and easy to implement.

AOPs involve chemicals that generate hydroxyl radicals to oxidize organic matter (Honarmandrad et al. 2022). The highly reactive hydroxyl radicals can convert impurities into water, inorganic ions, and carbon dioxide (Glaze et al. 1987).  $\bullet\text{OH}$  and  $\text{SO}_4^{\bullet-}$  are potent oxidizing radicals with redox potentials ( $E^\circ$ ) equal to 2.8 V and 2.5–3.1 V, respectively, which can rapidly and non-selectively oxidize and decompose most organic compounds in wastewater

(Babuponnusami and Muthukumar 2014; Lee et al. 2020). These two radicals are the primary oxidants responsible for the excellent performance of AOPs compared to conventional treatments (Xiao et al. 2017). When ozone is dissolved in an aqueous persulfate solution, it leads to the generation of a substantial amount of hydroxyl radicals ( $\bullet\text{OH}$ ). The produced  $\bullet\text{OH}$  activates the persulfate and generates  $\text{SO}_4^{\bullet-}$ ; the two oxidizing agents act synergistically in the system, improving the treatment efficiency of the system (Amr et al. 2013). The high DOM in wastewater competes with PMS for  $\text{O}_3$  to produce  $\bullet\text{OH}$ . Additionally,  $\text{O}_3$  exhibits excellent de-colorization and decomposition properties for challenging-to-degrade pollutants through both direct oxidation via  $\text{O}_3$  and indirect oxidation via free radicals (Wang et al. 2022); the  $\text{O}_3$ -PMS process is attractive because of its good stability (Yang et al. 2015).

The application research of  $\text{O}_3$ -PMS coupled catalytic oxidation process in petrochemical wastewater is still blank, and it is mostly used in domestic wastewater and degradation research of new pollutants, as shown in Table 1. This study investigated the efficiency of organic matter removal from petrochemical wastewater by the  $\text{O}_3$ -PMS coupled catalytic oxidation process. The degradation pathway and degradation efficiency of soluble organic matter by advanced oxidation technology were investigated to provide a basis for its further application in practical industrial wastewater treatment. Furthermore, the reactive radicals involved were trapped and identified via quenching experiments to understand the mechanism of radical interactions in the  $\text{O}_3$ -PMS system. Finally, the optimal reaction parameters for the  $\text{O}_3$ -PMS coupled catalytic oxidation were identified for economic evaluation.

## Materials and methods

### Experimental setup

Triangular wash bottles filled with water samples were placed in a magnetic rotor under the action of the magnetic stirrer as shown in Fig. 1. The water sample to be treated was added to each of the three triangular washing bottles. PMS was added to the samples in wash bottles a and c, following

**Table 1** Comparison of treatment effect of different wastewater by  $\text{O}_3$ -PMS process

Wastewater Source	COD <sub>Cr</sub> /TOC removal rate	References
landfill leachate	72%	Amr et al. (2013)
Ciproxacin	70%	Li et al. (2022)
Ibuprofen (IBP)	60%	Chen et al. (2024)

**Fig. 1** Experimental schematic diagram showing the experimental setup

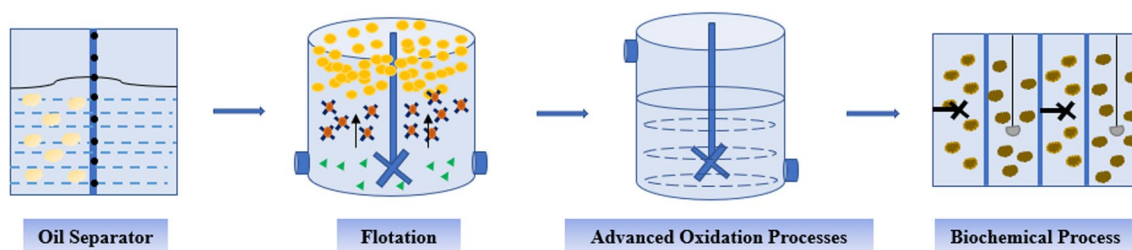
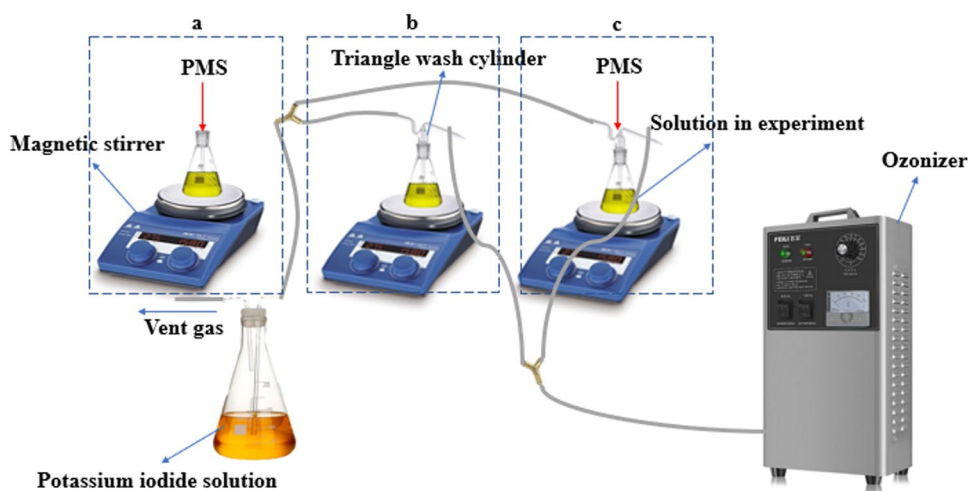
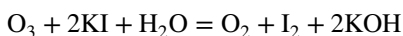


**Fig. 2** Petrochemical wastewater treatment process

which they were mixed thoroughly. Next, the ozone reactor fed ozone to the two triangular wash bottles b and c. The gaseous ozone is reduced to  $O_2$  upon entering the flasks by potassium iodide solution (see equation below).



### Source of water samples

The experimental water samples were obtained from the catalyst workshop of Yueyang petrochemical plant in Hunan Province, China. This petrochemical plant primarily produces catalysts used in chemical processing and the production of petrochemicals. Consequently, the plant consumes a lot of water, generating substantial amounts of petrochemical wastewater. Petrochemical wastewater treatment process is shown in Fig. 2.

Some indexes of water quality are shown in Table 2. The initial COD<sub>Cr</sub> (chemical oxygen demand) of the experimental wastewater water samples was  $75,000 \pm 500$  mg/L; the TOC (initial organic carbon) was  $30,000 \pm 300$  mg/L, whereas the total nitrogen content (ammonia nitrogen, nitrite nitrogen) was 300 mg/L or less. The chemical composition was highly complex. Since the chemical components could

**Table 2** Initial water sample index

Sample index	Numerical value
pH	$11 \pm 0.1$
EC ( $\mu\text{s}/\text{cm}$ )	$1215 \pm 10$
COD <sub>Cr</sub> (mg/L)	$75,000 \pm 500$
TOC (mg/L)	$30,000.00 \pm 300$
NH <sub>3</sub> -N (mg/L)	$30.45 \pm 0.50$
TN (mg/L)	$289.00 \pm 2.00$
NO <sub>2</sub> -N (mg/L)	$39.00 \pm 2.00$
NO <sub>2</sub> (mg/L)	$10.00 \pm 1.00$

not be entirely determined, COD<sub>Cr</sub> was analyzed to determine the efficacy of the treatment. When the water samples were brought to the laboratory, the oil and large particles in the water were removed by vacuum filtration. The filtered water samples were used for subsequent experiments.

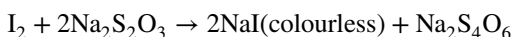
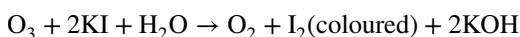
### Test method for removal of soluble organic matter

Petrochemical wastewater (200 mL) at room temperature ( $20 \sim 25$  °C) was taken for soluble organic matter degradation experiments. COD<sub>Cr</sub> was used as the index of soluble organic matter removal rate. The wastewater water samples

were filtered and added into a conical flask for ozone treatment in an ozone generator (CF-YG60, Shanmei Shumei, China). A gas flow meter monitored the reactor effluent's ozone concentration. Catalytic degradation of soluble organic matter was initiated when ozone and PMS were added to the conical flask. A magnetic stirrer mixed the solution at a constant stirring speed (180 r/min). Samples were removed at specified times and set aside for 6 h to maintain stability under ambient conditions. After the samples were dissolved through a dissolution apparatus, a UV spectrophotometer (UV-3600Plus, Shimadzu, Japan) was used to measure its COD<sub>Cr</sub>. The total organic carbon/total nitrogen analyzer (MULTIN/C2100, Jena, Germany) measured the TOC in the water samples. Parallel testing was conducted on multiple samples, and each degradation experiment was repeated three times to ensure reliability, with the average value being calculated.

### Method for determination of ozone concentration

The ozone concentration was determined through iodimetry, wherein ozone, exhibiting strong oxidation properties, reacts with an aqueous solution of potassium iodide to produce iodine. Subsequently, the generated iodine is titrated with a standard solution of sodium thiosulfate to sodium iodide, with the endpoint being the complete fading of the solution (Kasprzyk-Hordern et al. 2003). The reaction formula is as follows:



KI solution (20%, 20 mL) and deionized water (350 mL) were poured into a 500-mL iodine measuring bottle. After stable operation of the ozone generator, the gas flow is controlled at 0.4 L/min, and the gas is passed into a 500-mL iodine bottle containing 20% potassium iodide solution for 5 min. Then, 5-mL (1 + 5) sulfuric acid solution (pH 2) was added, and the bottle was plugged. After thorough mixing, it was left to stand for 5 min away from light. It was then titrated with 0.01 mol/L sodium thiosulfate standard solution until the solution was light yellow. Then, a few drops (about 1 mL) of 1% starch indicator were added and the titration was continued until the blue color just disappeared. The volume of sodium thiosulfate standard solution consumed was recorded. The ozone concentration can be calculated as follows:

$$C_{\text{O}_3}(\text{mg/L}) = \frac{2400 \cdot C_{\text{Na}} \cdot V_{\text{Na}}}{V_{\text{O}_3}}$$

Formula:

$C_{\text{O}_3}$  ozone concentration, mg/L;

$V_{\text{Na}}$  sodium thiosulfate solution volume used, mL;

$C_{\text{Na}}$  sodium thiosulfate solution concentration, mol/L;

$V_{\text{O}_3}$  amount of incoming ozone gas, mL.

### Methods of analysis of organic substances

The changes in major organic pollutants in water were characterized using a fluorescence spectrophotometer (F-7100, Hitachi, Japan). The changes in total organic carbon (TOC) in water were measured using a total organic carbon/total nitrogen (TOC/TN) analyzer. The non-polar and weakly polar DOM were detected using a 7890-B gas chromatograph 5977 B mass spectrometer (Agilent, Santa Clara, USA) equipped with an HP-5 column (30 m × 250 μm × 0.25 μm, Agilent, Santa Clara, USA). DOM was detected by liquid–liquid extraction (LLE) method using dichloromethane (DCM, HPLC grade) (Ge et al. 2022). The extract was dehydrated by anhydrous sodium sulfate. The temperature of the GC oven was set to 60 °C for 1 min, then increased to 290 °C at a rate of 8 °C/min, and held for 5 min. The temperature was rapidly increased to 320 °C at a rate of 2 °C/min and held for 7 min. The operational parameters of the mass spectrometer aligned with the methodology employed by Ye et al. (2021). Quenching experiments were carried out to confirm the role of free radicals and identify the optimal conditions for the determination of COD<sub>Cr</sub> in the coupled O<sub>3</sub>-PMS catalytic oxidation system.

## Results and discussion

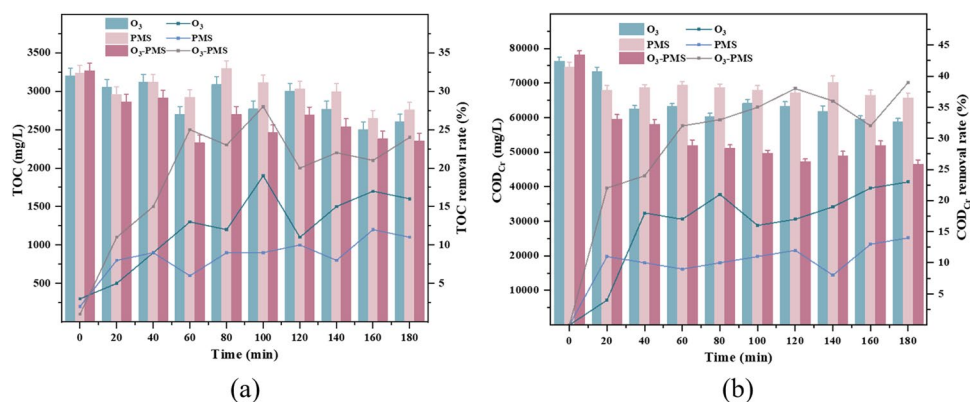
### Investigation of the effect of O<sub>3</sub>-PMS coupled catalytic oxidation on organic matter removal

#### TOC and COD<sub>Cr</sub> removal effect analysis

The wastewater was oxidized by ozone (ozone concentration was 25 mg/L), persulfate oxidation (persulfate dosage was 0.01 mol/L), and O<sub>3</sub>-PMS oxidation (ozone concentration was 25 mg/L, and persulfate dosage was 0.01 mol/L), respectively. The plot of COD<sub>Cr</sub> removal rate in wastewater versus time (Fig. 3b) revealed that the O<sub>3</sub>-PMS had the best removal effect. The TOC removal plot also demonstrated the same result.

From the experimental results, it can be seen that O<sub>3</sub>-PMS oxidation can attain 60% and 40% removal of TOC and COD<sub>Cr</sub>, respectively, indicating that they have a higher efficiency of wastewater treatment than ozone oxidation and

**Fig. 3** Comparison of **a** TOC and **b** COD<sub>Cr</sub> removal efficiency by three oxidation methods



persulfate oxidation methods. This increase in efficiency can be attributed to the synergistic effect of  $\bullet\text{OH}$  and  $\text{SO}_4^{\bullet-}$  in solution.

### Comparative analysis of three-dimensional fluorescence

Three-dimensional fluorescence data was collected by fluorescence photometry on the initially connected water samples, water samples oxidized by ozone (ozone concentration was 25 mg/L), water samples oxidized by peroxydisulfate (peroxydisulfate dosage was 0.01 mol/L), and water samples oxidized by O<sub>3</sub>-PMS (ozone concentration was 25 mg/L; peroxydisulfate dosage was 0.01 mol/L).

Three fluorescent components (C1–C3) were identified from the three-dimensional fluorescence spectra. C1, with Ex (excitation wavelength)/Em (emission wavelength) maxima at 230/330 nm, indicated the presence of aromatic hydrocarbons with bicyclic and tricyclic rings (Maqbool et al. 2020); C2, with Ex/Em maxima at 245/350 nm, corresponded to biodegradable compounds and bio-derivatives with complex structures (i.e., three and four aromatic rings) (Li et al. 2008; Yu et al. 2020; Zito et al. 2020); and C3, with Ex/Em maxima at 210/325 nm, showed two peaks representing phenolic compounds and/or naphthenic acids with one ring (Ge et al. 2022; Remolina et al. 2022).

The three-dimensional fluorescence diagram reveals that the original water sample (b) has a high C1, C2, and C3 content. The original water sample contains several components, such as aromatic hydrocarbons, biodegradable compounds, cyclic compounds, and other soluble organic compositions. The complex composition of the water renders the treatment difficult. When the water sample undergoes ozone treatment alone, as depicted in Fig. 4b, a significant reduction in impurities, including aromatic hydrocarbons, biodegradable compounds, cyclic compounds, and other soluble organic components, is observed compared to the original water samples. However, despite the evident removal effect with ozone treatment, a small portion of other organic components is generated, possibly resulting from the degradation

of large organic molecules into smaller ones under ozone oxidation. Persulfate oxidation occurred when only persulfate was added to the water samples (see Fig. 4c). Compared with the original water samples, part of the soluble organic matter in the water samples was also removed. However, the removal effect was still not obvious as other organic components were also produced. Given that peroxydisulfate oxidation involves large organic molecules, the organic matter is degraded into smaller molecules. When the water samples were treated with ozone and persulfate (Fig. 4d), most of the soluble organic matter in the water samples was removed compared with the original water samples. In comparison to ozone oxidation and peroxydisulfate oxidation, the O<sub>3</sub>-PMS oxidation system demonstrates more significant removal of soluble organic matter. It generates fewer additional small organic molecules, indicating a synergistic effect between the O<sub>3</sub>-PMS oxidation system, ozone, and peroxydisulfate. Persulfate exhibits a mutually synergistic effect, consistent with the study of Amr et al. (2013).

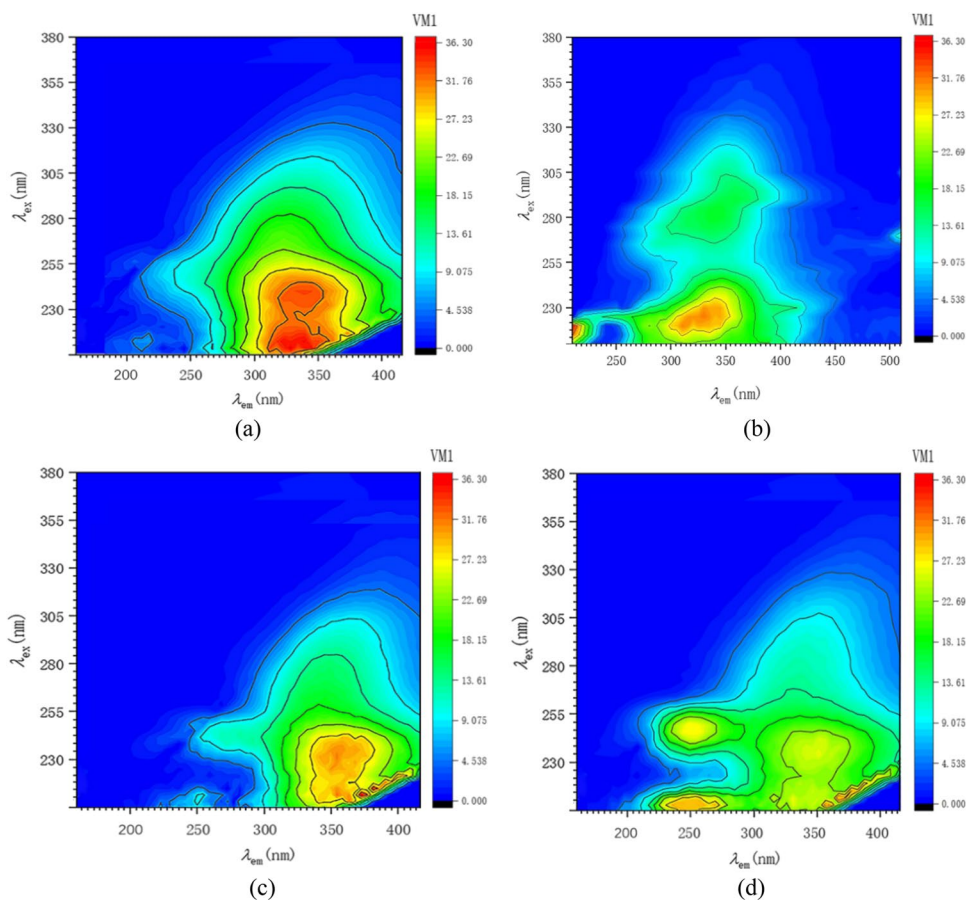
### Transition metal ion selection

The organic matter degrading efficiency of the O<sub>3</sub>-PMS system was further improved by adding transition metal ions. The metal ions catalyzed the system by activating the persulfate.

When the ozone concentration was 25 mg/L and persulfate dosing was 0.01 mol/L, transition metal ion compounds were added. The dosage of transition metal ion compounds (FeSO<sub>4</sub>, CuSO<sub>4</sub>, MnSO<sub>4</sub>, and ZnSO<sub>4</sub>) was 0.05 mol/L. The metal compounds were added to the coupled system to reduce the cost of the process.

As obvious from the experimental results, the catalytic efficiency of Fe<sup>2+</sup> and Cu<sup>2+</sup> compounds were the best. In the homogeneous system, the catalytic ability of mixed metal ions was greater than that of a single metal. The best transition metal ion combination for the two-two mixing was determined by the following experiment: the ozone concentration was maintained at 25 mg/L, the persulfate dosage

**Fig. 4** Three-dimensional fluorescence comparison of **a** initial water sample; **b** ozone oxidation; **c** persulfate oxidation; **d** O<sub>3</sub>-PMS coupled catalytic oxidation experiment



was 0.01 mol/L, and the dosage of multiple transition metals was 0.05 mol/L. Figure 5 b shows the experimental results. Fe<sup>2+</sup> and Cu<sup>2+</sup> metal ion compounds were selected for the best catalytic effect. Due to the addition of persulfate, the solution is acidic. However, it was not necessary to control the pH as a previous study (De Oliveira et al.2017) pointed out that the metal ion dissolution was higher at lower pH. Additionally, the TOC removal rate showed a positive correlation with the presence of metal ions, indicating a greater transformation from a non-homogeneous to a homogeneous reaction system, thereby enhancing pollutant removal. Moreover, the coupled system outperformed ozone alone, overcoming the limitation of ozone catalytic oxidation's weak oxidation ability at low pH. Consequently, the impact of pH on the O<sub>3</sub>-PMS coupled catalytic oxidation system was not investigated.

### Study of the O<sub>3</sub>-PMS coupled catalytic oxidation system

#### O<sub>3</sub>-PMS coupled catalytic oxidation of free radicals

O<sub>3</sub>-PMS coupled catalytic oxidation systems, usually involving ·OH and SO<sub>4</sub><sup>-</sup>·, were subjected to free radical

quenching experiments to elucidate the role of free radicals. TBA (thiobarbituric acid) is usually used as a ·OH quenching agent only, and EtOH (ethanol) can quench ·OH and SO<sub>4</sub><sup>-</sup>· (Kong et al.2019; Yu et al.2019). The addition of TBA to the O<sub>3</sub>-PMS coupled catalytic oxidation system resulted in a decrease in the degradation efficiency of organic matter. Similarly, the inclusion of EtOH also lowered the degradation efficiency, affirming the significant roles of ·OH and SO<sub>4</sub><sup>-</sup>· in the reaction system. The potential effect of superoxide radicals (·O<sub>2</sub><sup>-</sup>) must also be considered in the O<sub>3</sub>-PMS coupled catalytic oxidation system. Experiments with Nitrotetrazolium Blue Chloride NBT showed that there was no change in absorbance at 530 nm, indicating that NBT did not react with superoxide radicals (·O<sub>2</sub><sup>-</sup>) during the reaction (Bielski et al.1980; Zheng et al.2022). The results suggest that ·O<sub>2</sub><sup>-</sup> radicals may not be present in the O<sub>3</sub>-PMS coupled catalytic oxidation system. Benzoquinone (BQ) was added as a selective quenching agent for ·O<sub>2</sub><sup>-</sup> (Fan et al.2019; Zhang et al.2018; Zheng et al.2022). However, it showed only minimal inhibition of the degradation of soluble organic matter when its concentration was increased to 20 mM. The above findings exclude the effect of ·O<sub>2</sub><sup>-</sup> in the coupled O<sub>3</sub>-PMS catalytic oxidation system.

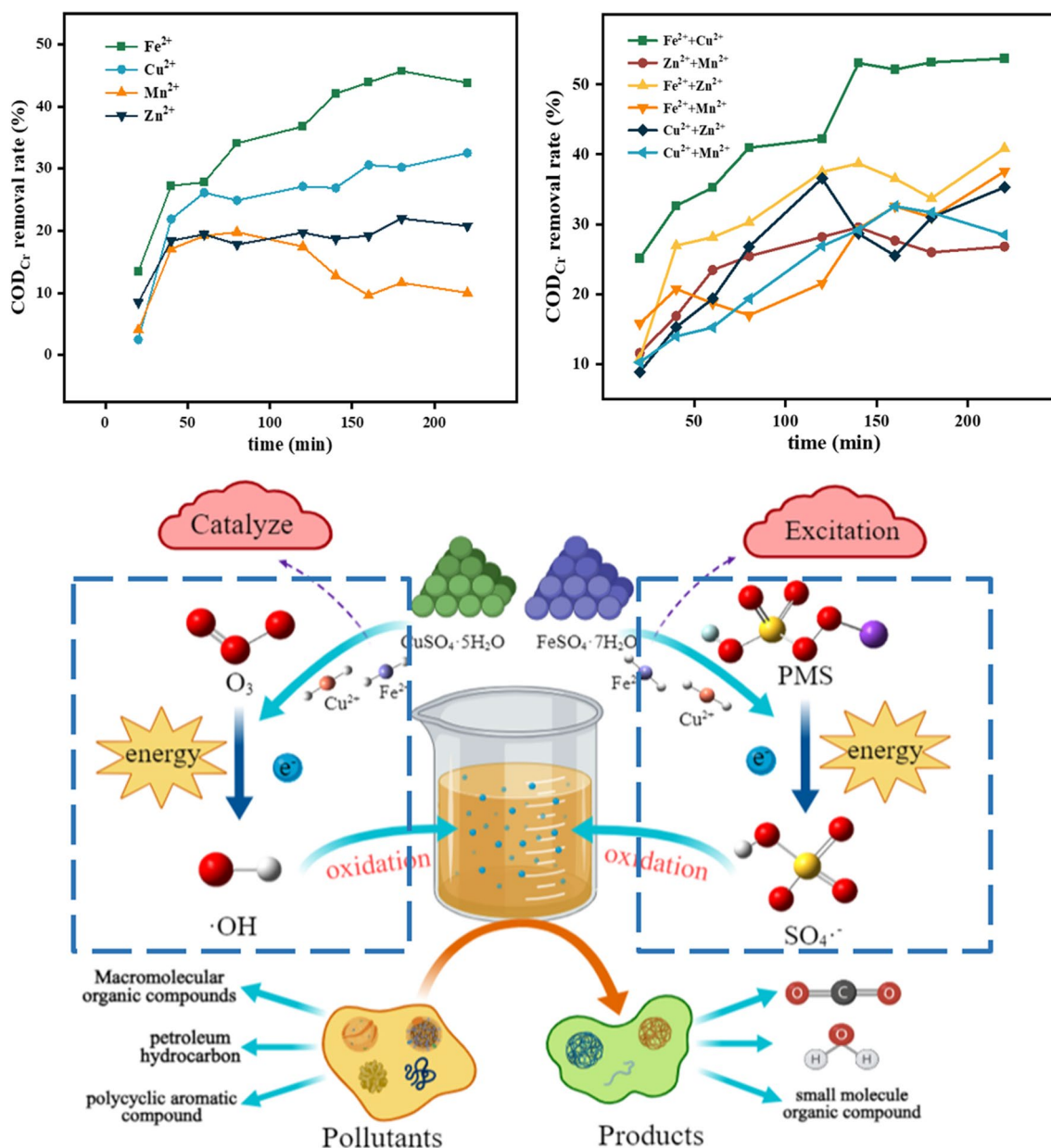


**Fig. 5** Role of transition metal ions on the coupled O<sub>3</sub>-PMS coupled catalytic oxidation system: **a** effect of single transition metal ion on O<sub>3</sub>-PMS system; **b** effect of multiple transition metal ions on O<sub>3</sub>-PMS system

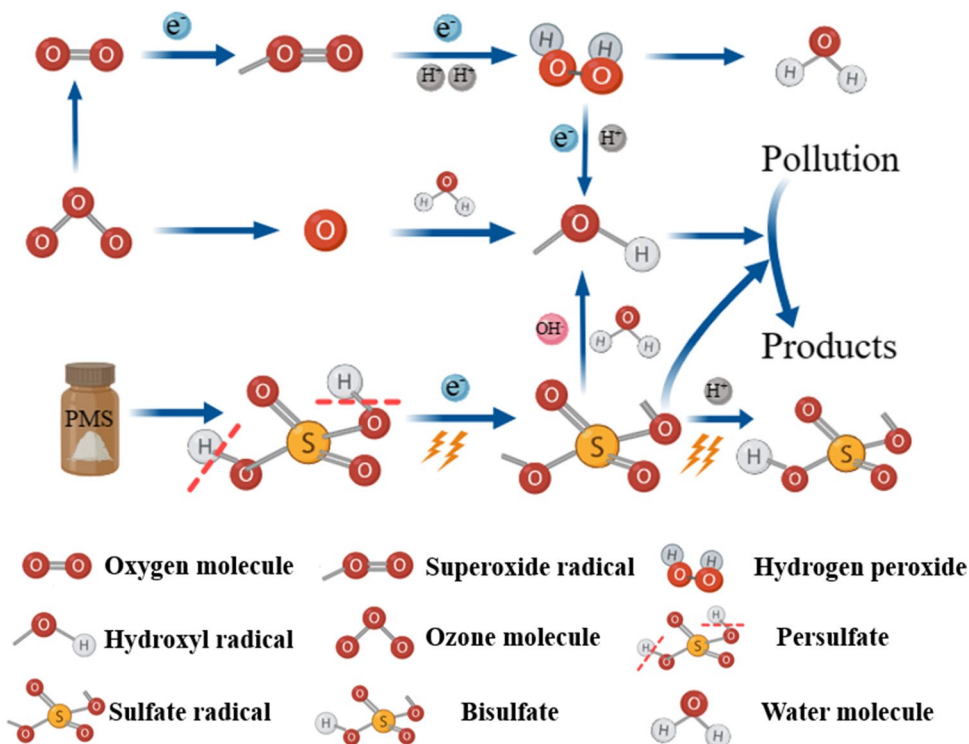
In the O<sub>3</sub>-PMS coupled catalytic oxidation system, the •OH and SO<sub>4</sub><sup>•-</sup> act synergistically, as seen in Fig. 6. •OH activates PMS, which induces PMS to produce SO<sub>4</sub><sup>•-</sup> in solution. Furthermore, when ozone is dissolved in an aqueous PMS solution, more •OH is produced (Eq. 3).



#### Investigation of the effect of transition metal ions in O<sub>3</sub>-PMS coupled catalytic oxidation systems

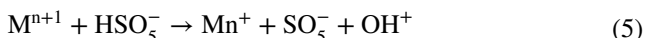
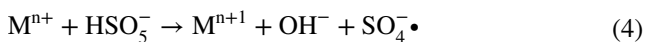
Removing soluble organic matter by the O<sub>3</sub>-PMS coupled catalytic oxidation system was not obvious without the addition of any metal ions. However, the addition of four different ions had varying impacts on the removal efficiency of the O<sub>3</sub>-PMS coupled catalytic oxidation system for soluble

**Fig. 6** Interaction between  $\bullet\text{OH}$  and  $\text{SO}_4^{\bullet-}$



organic matter. When the four ions were mixed two at a time, the combination of  $\text{Fe}^{2+}$  and  $\text{Cu}^{2+}$  exhibited the most effective synergistic effect.

During the metal ion catalysis process, most of  $\text{HSO}_5^-$  can react with metal ions to produce a large amount of  $\text{SO}_4^{\bullet-}$ :



High concentrations of metal ions generate large amounts of oxidants and free radicals in PMS to facilitate the degradation of soluble organic matter. However, the degradation efficiency of soluble organic matter exhibited a gradual increase with higher metal ion concentrations, primarily limited by the concentration of PMS (Zhao et al. 2017).

### Study of optimal reaction conditions for $\text{O}_3$ -PMS coupled catalytic oxidation

#### Orthogonal experimental design

A certain amount (0.05–0.15 mol/L) of transition metal ion ( $\text{Fe}^{2+}$  and  $\text{Cu}^{2+}$ ) mixture was added to the  $\text{O}_3$ -PMS coupled system. Orthogonal experiments were conducted as shown in Table 3, and the data were analyzed for four factors: ozone concentration (5~25 mg/L), persulfate dosage (0.01~0.05 mol/L), transition metal ion dosage ratio

(0:0, 0:1, 1:0, 2:1, 1:2), and reaction time (0~2 h), with five levels set (Fig. 7). This orthogonal analysis method was implemented following a previous study (Shang et al. 2022). The range analysis of the  $\text{O}_3$ -PMS coupled catalytic oxidation system via orthogonal experiments has been shown in Table 4.

Calculation of polar deviation:

$$K_i = \sum_{i=1}^n x_i$$

$$k_i = \frac{K_i}{n}$$

$$R = K_{max} - K_{min}$$

wherein

$K_i$  the sum of the results of the five trials corresponding to the  $i$ th level of the factor in the column;  $i$  is the number of levels under each factor.

$k_i$  mean value of  $K_i$ ;

$n$  number of levels under each factor;

$K_{max}$  maximum value of the column  $k_i$ ;



**Table 3** Orthogonal experiment on reaction conditions of O<sub>3</sub>-PMS coupled catalytic oxidation system

Serial number	Ozone concentration (mg/L)	Dosage of persulfate(mol/L)	Transition metal ion dosing ratio	Response time (h)	COD <sub>Cr</sub> removal rate (%)
1	5	0.01	0: 1	0.0	0
2	5	0.02	1: 0	0.5	48.41
3	5	0.03	1: 1	1.0	51.91
4	5	0.04	1: 2	1.5	13.47
5	5	0.05	2: 1	2.0	32.78
6	10	0.02	1: 1	1.5	37.64
7	10	0.03	1: 2	2.0	52.71
8	10	0.04	2: 1	0.0	17.96
9	10	0.05	0: 1	0.5	29.06
10	10	0.01	1: 0	1.0	36.91
11	15	0.03	2: 1	0.5	19.65
12	15	0.04	0: 1	1.0	17.43
13	15	0.05	1: 0	1.5	24.62
14	15	0.01	1: 1	2.0	35.14
15	15	0.02	1: 2	0.0	5.96
16	20	0.04	1: 0	2.0	16.75
17	20	0.05	1: 1	0.0	30.63
18	20	0.01	1: 2	0.5	28.03
19	20	0.02	2: 1	1.0	36.26
20	20	0.03	0: 1	1.5	11.5
21	25	0.05	1: 2	1.0	18.7
22	25	0.01	2: 1	1.5	66.86
23	25	0.02	0: 1	2.0	51.62
24	25	0.03	1: 0	0.0	12.16
25	25	0.04	1: 1	0.5	8.85

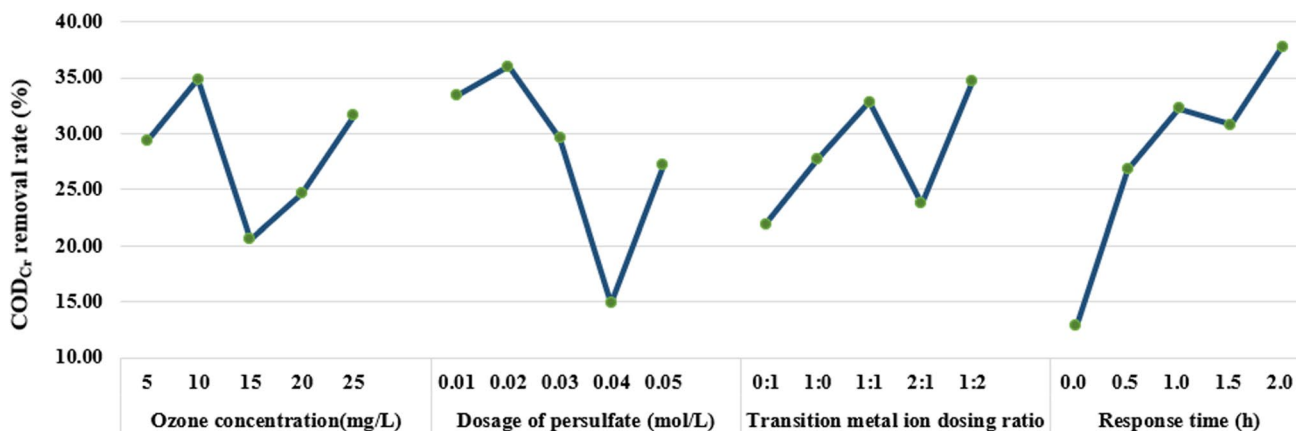


**Fig. 7** Orthogonal experimental effects of the O<sub>3</sub>-PMS coupled catalytic oxidation system

$K_{min}$  The minimum value of the column  $k_i$ .

The polar analysis results show that the order of factors is as follows: reaction time > peroxydisulfate dosage > ozone concentration > transition metal ion dosage ratio.

Based on the extreme difference analysis, the effect curve is depicted in Fig. 8. The orthogonal experimental effect plot indicates that the oxidation efficiency was poorest at an ozone concentration of 15 mg/L, resulting in the lowest average COD<sub>Cr</sub> removal efficiency. The

**Table 4** Range analysis table of O3-PMS coupled catalytic oxidation system via orthogonal experiments

Extremum	Element			
	Ozone discharge (L/min)	Dosage of persulfate (mol/L)	Transition metal ion dosing ratio	Response time (h)
$K_1$	146.57	166.94	109.61	64.11
$K_2$	174.28	179.89	138.85	134
$K_3$	102.8	147.93	164.17	161.21
$K_4$	123.17	74.46	118.87	154.09
$K_5$	158.19	135.79	173.51	189
$k_1$	29.314	33.388	21.922	12.822
$k_2$	34.856	35.978	27.77	26.8
$k_3$	20.56	29.586	32.834	32.242
$k_4$	24.634	14.892	23.774	30.818
$k_5$	31.638	27.158	34.702	37.8
Range	14.296	21.086	12.78	24.978

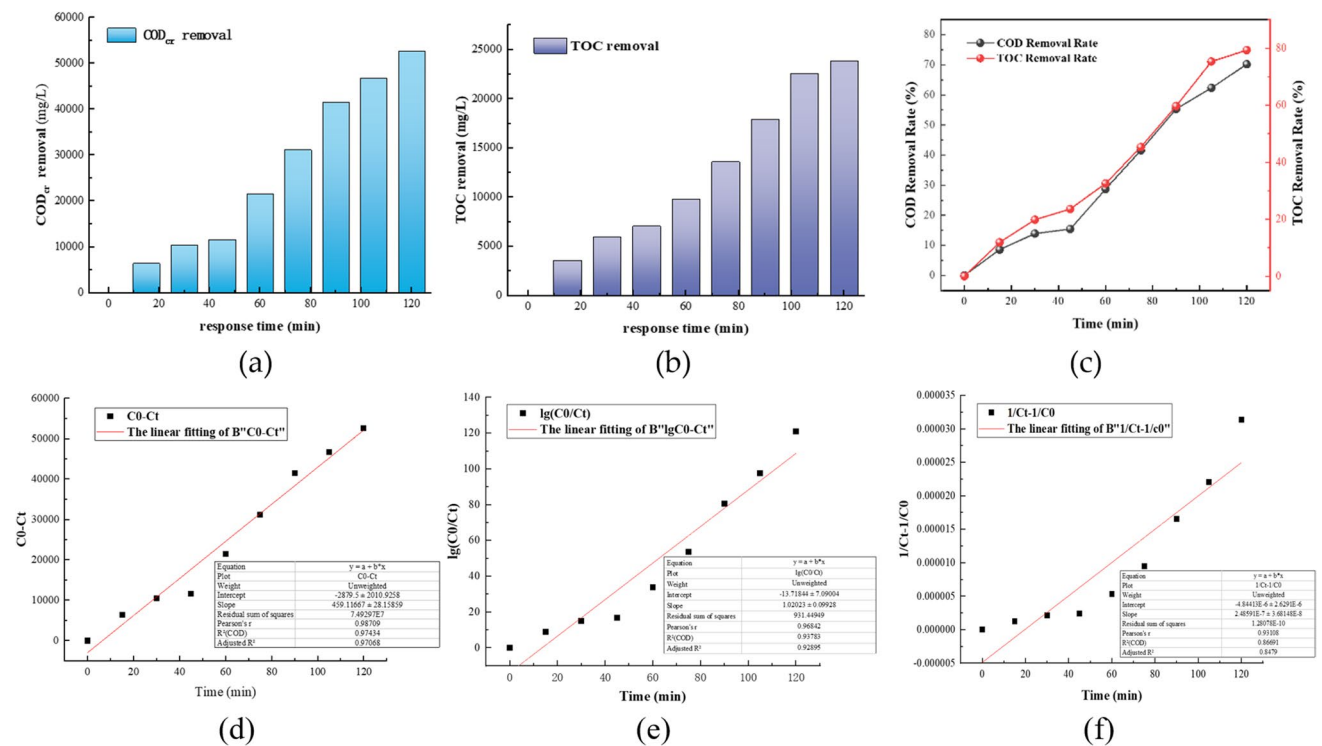


**Fig. 8** Reaction kinetics analysis: **a** COD<sub>Cr</sub> removal; **b** TOC removal; **c** COD<sub>Cr</sub>/TOC removal rate; **d** zero-order reaction kinetics; **e** first-order reaction kinetics; **f** second-order reaction kinetics

best reaction was achieved when the ozone concentration was 10 mg/L. Normally, the degradation rate of target pollutants by ozone in wastewater is influenced by the mass transfer of ozone. This, in turn, is connected to the decomposition kinetics of ozone in water, as well as the quantity and size of ozone bubbles generated (Chu et al.2007; Mitani et al.2005). At an ozone concentration of 10 to 15 mg/L, the COD<sub>Cr</sub> removal efficiency decreased because as the ozone concentration increased, the volume

of bubbles in the reactor increased, affecting the mass transfer efficiency of ozone. On the contrary, at lower concentrations, the rapid generation of small bubbles during rupture expedited the indirect oxidation process of ozone, leading to the production of numerous hydroxyl radicals. This acceleration contributed to the degradation of organic pollutants and resulted in the degradation of organic pollutants from large molecular pollutants to small molecular pollutants or even complete degradation to CO<sub>2</sub> and

**Table 5** Correlation analysis of fitted curves for O<sub>3</sub>-PMS coupled catalytic oxidation process

Reaction order	Fitted equation	Intercept	Slope	Linearly dependent coefficient ( $R^2$ )
Zero-order	$y = a + b * x$	-2879.5	459.12	0.97434
First-order	$y = a + b * x$	-13.72	1.02	0.93783
Second-order	$y = a + b * x$	-4.84	2.49	0.93108

**Table 6** Water quality indices of O<sub>3</sub>-PMS coupled catalytic oxidation system treated under optimal reaction conditions

Sample index	Numerical value
pH	5.0 ± 0.1
EC (μs/cm)	450 ± 10
COD <sub>Cr</sub> (mg/L)	22,000 ± 100
TOC (mg/L)	6200.00 ± 20
NH <sub>3</sub> -N (mg/L)	18.32 ± 0.50
TN (mg/L)	29.30 ± 0.50
NO <sub>2</sub> -N (mg/L)	5.00 ± 0.10
NO <sub>2</sub> (mg/L)	1.00 ± 1.00

H<sub>2</sub>O (Chu et al. 2007; Hernández et al. 2022; Alimoradi and Stohr 2020). When the ozone concentration was 15 to 25 mg/L, the COD<sub>Cr</sub> removal rate continued to increase with the ozone concentration due to the synergistic effect of ozone and persulfate in this coupled system.

The least effective COD<sub>Cr</sub> removal was observed at a persulfate dosage of 0.04 mol/L, while the most efficient COD<sub>Cr</sub> removal occurred at a persulfate dosage of 0.02 mol/L. This disparity in removal efficiency can be mainly attributed to the constraint resulting from persulfate concentration. The highest and lowest average COD<sub>Cr</sub> removal efficiencies were attained at transition metal ion dosing ratios of 1:2 and 0:1, respectively. The oxidation efficiency was optimum when the reaction time was 2.0 h (Table 5). Thus, the COD<sub>Cr</sub> removal efficiency positively correlated with the reaction time. These orthogonal experimental results showed that the optimal removal conditions of COD<sub>Cr</sub> were as follows: ozone concentration of 10 mg/L, persulfate dosage of 0.02 mol/L, Fe<sup>2+</sup>: Cu<sup>2+</sup> ion dosage ratio of 1:2, and a reaction time of 2 h.

The water quality indices of the O<sub>3</sub>-PMS coupled catalytic oxidation system treated under optimal removal conditions of COD<sub>Cr</sub> are shown in Table 6. Post O<sub>3</sub>-PMS treatment under the optimal reaction conditions, the COD<sub>Cr</sub> and TOC removal rates reached 70% and 79.3%, respectively. Furthermore, the TN and NH<sub>3</sub>-N levels could be reduced to less than 30 mg/L. These rates were achieved under the optimal reaction conditions of O<sub>3</sub>-PMS, resulting in a TOC removal rate of 79.3%.

## Kinetic analysis of O<sub>3</sub>-PMS coupled catalytic oxidation reaction

The experimental results are modeled using the COD removal rate as the index and fit into kinetic equations (Ahmadi et al. 2016). Typically, the simulated degradation process is described by zero-order, first-order, and second-order kinetic equations. In the process of O<sub>3</sub>-PMS coupled catalytic oxidation treatment of petrochemical wastewater, samples were taken at 0, 15, 30, 45, 60, 75, 90, 105, and 120 min. Zero-order, first-order, and second-order reaction kinetics equations were adopted, with  $C_0 - C_t$ ,  $\ln(C_0/C_t)$ ,  $1/C_t - 1/C_0$  as the ordinate and time  $t$  as the abscissa, respectively. Reaction kinetics fitting was performed. The linear expression equations are as follows:

$$C_0 - C_t = k_0 t$$

$$\ln\left(\frac{C_0}{C_t}\right) = k_1 t$$

$$\frac{1}{C_t} = k_2 t + \frac{1}{C_0}$$

wherein

$C_0$  COD<sub>Cr</sub> concentration at the initiation of ozone-persulfate coupled catalytic oxidation reaction, mg/L.

$C_t$  COD concentration at time  $t$  in ozone-persulfate coupling catalytic oxidation reaction, mg/L.

$K_0$  zero-order rate constant of O<sub>3</sub>-PMS coupled catalytic oxidation reaction.

$K_1$  first-order kinetic rate constant of O<sub>3</sub>-PMS coupled catalytic oxidation reaction;

$K_2$  second-order rate constant O<sub>3</sub>-PMS coupled catalytic oxidation reaction;

According to the fitting results (Fig. 8; Table 5), the linear correlation coefficients ( $R^2$ ) obtained by linear fitting of zero-order, first-order, and second-order kinetics are 0.97434, 0.93783, and 0.93108, respectively. It can be seen that the COD<sub>Cr</sub> removal efficiency of O<sub>3</sub>-PMS coupled catalytic oxidation process basically conforms to the zero-order kinetic law.

**Table 7** Organic content in before processing wastewater water samples

Compound label	Retention time	Molecular formula
3-Heptanone	C <sub>7</sub> H <sub>14</sub> O	12.04
Cyclotetrasiloxane, octamethyl	C <sub>8</sub> H <sub>24</sub> O <sub>4</sub> Si <sub>4</sub>	5.03
Hexanoic acid,2-ethyl	C <sub>8</sub> H <sub>16</sub> O <sub>2</sub>	7.67
3,6-Heptanedione	C <sub>7</sub> H <sub>12</sub> O <sub>2</sub>	17.44
Pentanoic acid, 5-hydroxy-,2,4-di-t-butylphenyl esters	C <sub>19</sub> H <sub>30</sub> O <sub>3</sub>	14.11
Acetic acid,chloro-,octadecyl ester	C <sub>20</sub> H <sub>39</sub> ClO <sub>2</sub>	20.74
Phtjalic acid,di(2-propylpentyl)ester	C <sub>24</sub> H <sub>38</sub> O <sub>4</sub>	26.55

**Table 8** Organic content in after processing wastewater water samples

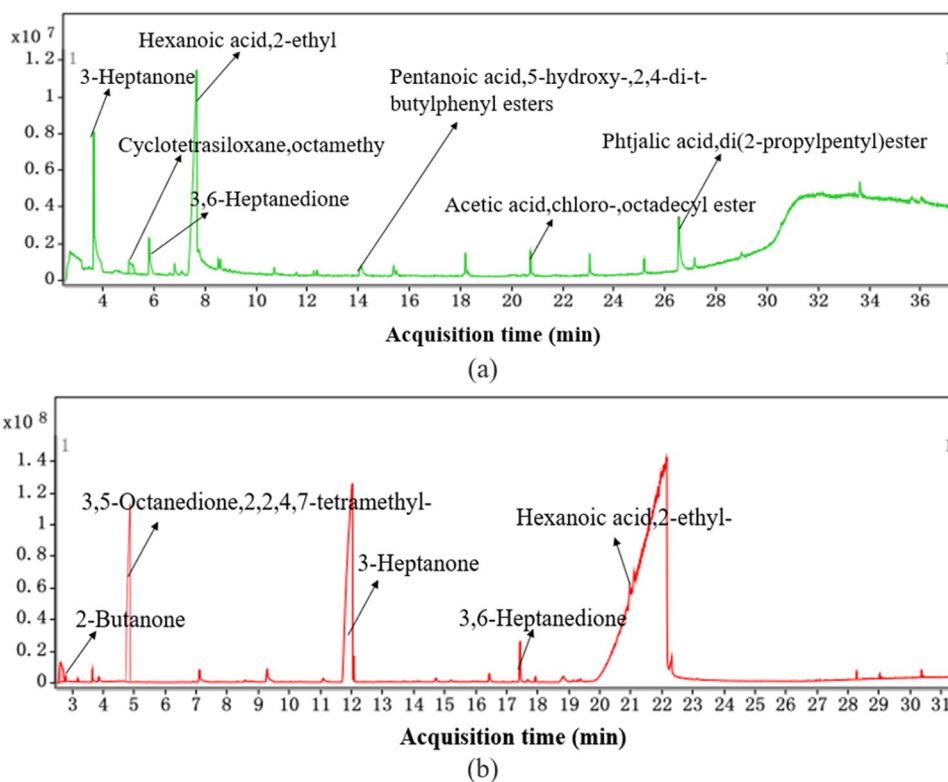
Compound label	Retention time	Molecular formula
2-Butanone	C <sub>4</sub> H <sub>8</sub> O	2.62
3,5-Octanedione,2,2,4,7-tetramethyl-	C <sub>12</sub> H <sub>22</sub> O <sub>2</sub>	3.65
3-Heptanone	C <sub>7</sub> H <sub>14</sub> O	12.04
3,6-Heptanedione	C <sub>7</sub> H <sub>12</sub> O <sub>2</sub>	17.44
Hexanoic acid,2-ethyl-	C <sub>8</sub> H <sub>16</sub> O <sub>2</sub>	7.67

## Gas chromatography-mass spectrometry (GC–MS) analysis

The petroleum hydrocarbons in wastewater were analyzed by gas chromatography-mass spectrometry (GC–MS). The GC–MS analysis indicated the presence of hydrocarbon and aromatic compounds in the water, as detailed in Tables 7 and 8. The application of the O<sub>3</sub>-PMS coupled catalytic oxidation method led to the removal or degradation of these identified compounds, providing additional confirmation of the effectiveness of the O<sub>3</sub>-PMS coupled catalytic oxidation process.

The GC–MS analysis of organic matter in water samples before and after the reaction, combined with three-dimensional fluorescence data (Fig. 4) was used to investigate the degradation mechanism of organic matter. The study inferred potential intermediate products and analyzed types of organic matter resistant to the O<sub>3</sub>-PMS coupled catalytic oxidation process. This analysis serves as a foundational step for further research. As shown in Figs. 9 and 10, the O<sub>3</sub>-PMS coupled catalytic oxidation can effectively degrade organic compounds such as tryptophan (C<sub>12</sub>H<sub>15</sub>N<sub>2</sub>O<sub>2</sub>) and tyrosine (C<sub>9</sub>H<sub>11</sub>NO<sub>3</sub>), as well as some aromatic compounds and hydrocarbons. It is however not successful in degrading organic compounds such as C<sub>8</sub>H<sub>16</sub>O<sub>2</sub>, C<sub>7</sub>H<sub>12</sub>O<sub>2</sub>, and C<sub>8</sub>H<sub>16</sub>O<sub>2</sub>, necessitating further treatment.

**Fig. 9** Initial water sample GC–MS processing diagram: **a** initial water sample GC–MS mass spectrometry; **b** GC–MS mass spectrum of water treated by O<sub>3</sub>-PMS coupled oxidation catalysis



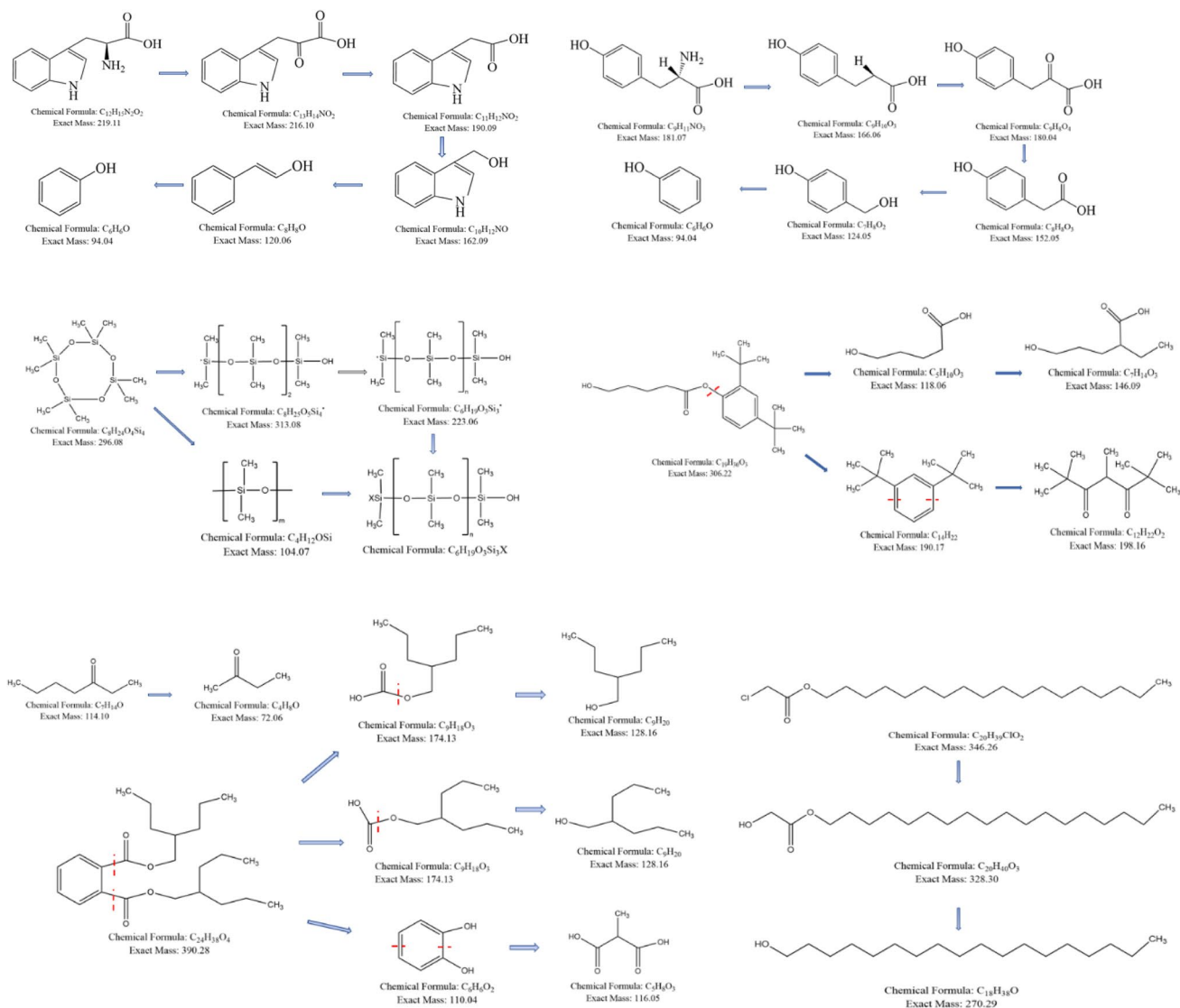


Fig. 10 Degradation pathway of soluble organic matter

## Cost evaluation of wastewater treatment

The  $COD_{Cr}$  removal efficiency was used to calculate the cost of wastewater treatment which was compared with those reported in previous studies (Wang et al. 2020; Cako et al. 2020). The  $O_3$ -PMS coupled catalytic oxidation system required specific energy inputs, including an ozone reactor, and persulfate and transition metal ions. The ozone reactors consumed 6 kW of electricity per hour, the PMS was priced at \$0.036 per gram, and the added metal cost was \$0.010 per gram. The wastewater treatment cost details are presented in Table 9.

The findings from this study suggest that  $O_3$ -PMS coupled catalytic oxidation is a cost-effective technology for

Table 9 Cost assessment

Process	$COD_{Cr}$ processing time (h)	Electricity cost/ $m^3$ (US \$)	Chemical cost/ $m^3$ (US \$)	Total cost/ $m^3$ (US \$)
$O_3$	5.0	0.35	0.00	0.35
PMS	2.0	0.00	0.098	0.098
$O_3$ -PMS	2.0	0.22	0.102	0.322

the treatment of petrochemical wastewater. Typically, it is applied upstream of the bioreactor to facilitate the breakdown of macromolecules into smaller ones, promoting absorption by microorganisms.

## Conclusions

In this study, O<sub>3</sub>-PMS exhibited significant advantages in the deep treatment of petrochemical wastewater. The optimal parameters, degradation mechanism, and economic evaluation of the catalytic process were investigated in this study. The best COD<sub>Cr</sub> removal was achieved at an ozone concentration of 20 mg/L, a persulfate dosage of 0.02 mol/L, a Fe<sup>2+</sup>: Cu<sup>2+</sup> dosage ratio of 1:2, and a reaction time of 2 h. The results of quenching experiments demonstrated that hydroxyl radicals and persulfate radicals had a critical role in the mixed system. In the presence of reactive species, complex molecules in challenging-to-degrade pollutants underwent fragmentation into smaller molecules, leading to their removal. O<sub>3</sub>-PMS coupled catalytic oxidation can effectively degrade aromatic and hydrocarbon compounds. Using the coupled O<sub>3</sub>-PMS catalytic oxidation system, the total cost of treating 1 m<sup>3</sup> of wastewater to achieve COD<sub>Cr</sub> ≤ 20,000 mg/L (COD<sub>Cr</sub> treatment rate of 70%) was calculated to be US\$0.322.

Overall, the O<sub>3</sub>-PMS coupled catalytic oxidation process is a cost-effective technology for advanced industrial wastewater treatment. In future research, the connection of multiple O<sub>3</sub>-PMS coupled catalytic oxidation reaction systems in series or parallel configurations could enhance treatment capacity and efficiency. Integrating additional O<sub>3</sub>-PMS coupled catalytic oxidation systems is anticipated to further enhance the COD<sub>Cr</sub> removal rate, ultimately meeting recommended wastewater discharge standards.

**Author contribution** Conceptualization, W. G.; methodology, W. G.; software, C. L.; validation, J. Z., Y. D., and Q. Y.; data curation, C. L., and Y. D.; writing—original draft preparation, J. Z.; writing—review and editing, W. G. and C. L.; visualization, Y. D. and Q. Y.; supervision, Q. Y. and H. G. All authors have read and agreed to the published version of the manuscript.

**Funding** The authors thank the Gansu Provincial Department of Education university scientific research innovation platform major cultivation project (2024GJPT), for providing the support.

**Data Availability** The data that support the findings of this study are available on request from the corresponding author, Q. Y., upon reasonable request.

## Declarations

**Ethics approval** Not applicable.

**Consent to participate** Not applicable.

**Consent for publication** Not applicable.

**Competing interests** The authors declare no competing interests.

## References

- Ahmadi M, Behin J, Mahnam AR (2016) Kinetics and thermodynamics of peroxydisulfate oxidation of Reactive Yellow 84. *J Saudi Chem Soc* 20(6):644–650
- Alimoradi S, Stohr H (2020) Stagg-Williams S (2020) Effect of temperature on toxicity and biodegradability of dissolved organic nitrogen formed during hydrothermal liquefaction of biomass. *Chemosphere* 238:124573
- Amr SS, Aziz HA, Adlan MN, Bashir MJK (2013) Pretreatment of stabilized leachate using ozone/persulfate oxidation process. *Chem Eng J* 221:492–499. <https://doi.org/10.1016/j.cej.2013.02.038>
- Babuponnsami A, Muthukumar K (2014) A review on Fenton and improvements to the Fenton process for wastewater treatment. *J Environ Chem Eng* 2:557–572. <https://doi.org/10.1016/j.jece.2013.10.011>
- Bielski BH, Shiue GG, Bajuk S (1980) Reduction of nitro blue tetrazolium by CO<sub>2</sub>-and O<sub>2</sub>-radicals. *J Phys Chem* 84:830–833. <https://doi.org/10.1002/chin.198030147>
- Cako E, Gunasekaran KD, Soltani RDC, Boczkaj G (2020) Ultrafast degradation of brilliant cresyl blue under hydrodynamic cavitation based advanced oxidation processes (AOPs). *Water Res Ind* 24:100134. <https://doi.org/10.1016/j.wri.2020.100134>
- Chen W, Tian Y, Liu D, Yi Y, Li X, Wang J, Bin L, Li P, Tang B, Li L (2024) Unveiling the mechanism of enhanced water purification by F-Fe-Zn-MCM-41 in O<sub>3</sub>/PMS. *Appl Catal B: Environ* 123608. <https://doi.org/10.1016/j.apcatb.2023.123608>
- Chu L, Xing X, Yu A (2007) Enhanced ozonation of simulated dye-stuff wastewater by microbubbles. *Chemosphere* 68:1854–1860
- De Oliveira AMD, Maniero MG, Rodrigues-Silva C, Guimarães JR (2017) Antimicrobial activity and acute toxicity of ozonated lomefloxacin solution. *Environ Sci Pollut Res* 24:6252–6260. <https://doi.org/10.1007/s11356-016-8319-0>
- Fan J, Qin H, Jiang S (2019) Mn-doped g-C<sub>3</sub>N<sub>4</sub> composite to activate peroxydisulfate for acetaminophen degradation: the role of superoxide anion and singlet oxygen. *Chem Eng J* 359:723–732. <https://doi.org/10.1016/j.cej.2018.11.165>
- Fernandes A, Gałol M, Makoś P (2019) Integrated photocatalytic advanced oxidation system (TiO<sub>2</sub>/UV/O<sub>3</sub>/H<sub>2</sub>O<sub>2</sub>) for degradation of volatile organic compounds. *Sep Purif Technol* 224:1–14
- Fernandes A, Makoś P, Wang Z (2020) Synergistic effect of TiO<sub>2</sub> photocatalytic advanced oxidation processes in the treatment of refinery effluents. *Chem Eng J* 391:123488
- Ge D, Wu W, Li G (2022) Application of CaO<sub>2</sub>-enhanced peroxide process to adjust waste activated sludge characteristics for dewaterability amelioration: Molecular transformation of dissolved organic matters and realized mechanism of deep-dewatering. *Chem Eng J* 437:135306. <https://doi.org/10.1016/j.cej.2022.135306>
- Glaze WH, Kang JW, Chapin DH (1987) The chemistry of water treatment processes involving ozone, hydrogen peroxide and ultraviolet radiation. *The Journal of the International Ozone Association* 9(4):335–352. <https://doi.org/10.1080/01919518708552148>
- Gopalakrishnan B, Bharathiraja B (2022) Experimental design approach for petrochemical waste water treatment using solar assisted photo Fenton process. *J Indian Chem Soc* 99:100622
- Hayati F, Isari AA, Fattahi M, Jorfi S (2018) Photocatalytic decontamination of phenol and petrochemical wastewater through ZnO/TiO<sub>2</sub> decorated on reduced graphene oxide nanocomposite: influential operating factors, mechanism, and electrical energy consumption. *RSC Adv* 8:40035–40053. <https://doi.org/10.1039/c8ra07936f>
- Hernández EV, Monje-Ramírez I, Velásquez-Orta SB (2022) Surface activity of biomolecules released from microalgae harvested by ozone-flotation. *Environ Tech Innov* 26:102354

- Honarmandrad Z, Sun X, Wang Z (2022) Activated persulfate and peroxymonosulfate based advanced oxidation processes (AOPs) for antibiotics degradation—a review. *Water Resour Ind* 100194. <https://doi.org/10.1016/j.wri.2022.100194>
- Kasprzyk-Hordern B, Ziólek M, Nawrocki J (2003) Catalytic ozonation and methods of enhancing molecular ozone reactions in water treatment. *Appl Catal B* 46(4):639–669
- Kong L, Fang G, Chen Y (2019) Efficient activation of persulfate decomposition by  $\text{Cu}_2\text{FeSnS}_4$  nanomaterial for bisphenol A degradation: kinetics, performance and mechanism studies. *Appl. Catal. B Environ.* 253:278–285. <https://doi.org/10.1016/j.apcatb.2019.04.069>
- Kumar N, Baudh K, Kumar S (2013) Extractability and phytotoxicity of heavy metals present in petrochemical industry sludge. *Clean Tech Environ Policy* 15:1033–1039
- Lee J, Von Gunten U, Kim JH (2020) Persulfate-based advanced oxidation: critical assessment of opportunities and roadblocks. *Environ Sci Tech* 54:3064–3081
- Li W, Sheng G, Liu X (2008) Characterizing the extracellular and intracellular fluorescent products of activated sludge in a sequencing batch reactor. *Water Res* 42:3173–3181
- Li S, Fan X, Gu M, Cagnetta G, Huang J, Yu G (2022) Confined-space strategy for anchoring catalytic nanoparticles on Si-OH by ball milling for enhanced  $\text{O}_3/\text{PMS}$  oxidation of ciprofloxacin. *Chem Eng J* 429:132318
- Liu S, Ma Q, Wang B (2014) Advanced treatment of refractory organic pollutants in petrochemical industrial wastewater by bioactive enhanced ponds and wetland system. *Ecotoxicology* 23:689–698
- Maqbool T, Qin Y, Ly QV (2020) Exploring the relative changes in dissolved organic matter for assessing the water quality of full-scale drinking water treatment plants using a fluorescence ratio approach. *Water Res* 183:116125. <https://doi.org/10.1016/j.watres.2020.116125>
- Mitani MM, Keller AA, Sandall OC (2005) Mass transfer of ozone using a microporous diffuser reactor system. *Ozone: Sci Eng* 27:45–51
- Remolina MC, Li Z, Peleato NM (2022) Application of machine learning methods for rapid fluorescence-based detection of naphthenic acids and phenol in natural surface waters. *J Hazard Mater* 430:128491. <https://doi.org/10.1016/j.jhazmat.2022.128491>
- Shang Y, Guan Y, Tang Z, Fang Z (2022) Characterization of runoff pollutant removal in biological retention systems by orthogonal experiment. *J Water Process Eng* 49:103145. <https://doi.org/10.1016/j.jwpe.2022.103145>
- Tian X, Song Y, Shen Z, Zou Y, Liu T (2020) A comprehensive review on toxic petrochemical wastewater pretreatment and advanced treatment. *J Clean Prod* 245:118692
- Tong K, Lin A, Ji G, Wang D (2016) The effects of adsorbing organic pollutants from super heavy oil wastewater by lignite activated coke. *J Hazard Mater* 308:113–119
- Wang F, Hao H, Sun R (2014) Bench-scale and pilot-scale evaluation of coagulation pre-treatment for wastewater reused by reverse osmosis in a petrochemical circulating cooling water system. *Desalination* 335:64–69
- Wang J, Chen H, Yuan R, Wang F, Zou B (2020) Intensified degradation of textile wastewater using a novel treatment of hydrodynamic cavitation with the combination of ozone. *J Environ Chem Eng* 8:103959. <https://doi.org/10.1016/j.jece.2020.103959>
- Wang D, Sun D, Tian X, Liu N, Wang S (2021) Role of microbial communities on organic removal during petrochemical wastewater biological treatment with pure oxygen aeration. *J Water Process Eng* 42:102151. <https://doi.org/10.1016/j.jwpe.2021.102151>
- Wang J, Yuan R, Feng Z (2022) The advanced treatment of textile printing and dyeing wastewater by hydrodynamic cavitation and ozone: degradation, mechanism, and transformation of dissolved organic matter. *Environ Res* 215:114300
- Xiao R, Gao L, Wei Z, Spinney R, Luo S (2017) Mechanistic insight into degradation of endocrine disrupting chemical by hydroxyl radical: an experimental and theoretical approach. *Environ Pollut* 231:1446–1452. <https://doi.org/10.1016/j.envpol.2017.09.006>
- Yang Y, Jiang J, Lu X (2015) Production of sulfate radical and hydroxyl radical by reaction of ozone with peroxymonosulfate: a novel advanced oxidation process. *Environ Sci Tech* 49:7330–7339
- Ye H, Chen L, Kou Y (2021) Influences of coagulation pretreatment on the characteristics of crude oil electric desalting wastewaters. *Chemosphere* 264:128531. <https://doi.org/10.1016/j.chemosphere.2020.128531>
- Yu M, Xi BD, Zhu ZQ (2020) Fate and removal of aromatic organic matter upon a combined leachate treatment process. *Chem Eng J* 401:126157. <https://doi.org/10.1016/j.cej.2020.126157>
- Yu Y, Tan P, Huang X, Li R, Wang N (2019) Homogeneous activation of peroxymonosulfate using a low-dosage cross-bridged cyclam manganese (II) complex for organic pollutant degradation via a nonradical pathway. *J Hazard Mater* <https://doi.org/10.1016/j.jhazmat.2019.03.002>
- Zhang C, Dong Y, Li B, Li F (2018) Comparative study of three solid oxidants as substitutes of  $\text{H}_2\text{O}_2$  used in Fe (III)-oxalate complex mediated Fenton system for photocatalytic elimination of reactive azo dye. *J Clean Prod* 177:245–253. <https://doi.org/10.1016/j.jclepro.2017.12.211>
- Zhao Z, Dong W, Wang H, Chen G, Wang H (2017) Advanced oxidation removal of hypophosphite by  $\text{O}_3/\text{H}_2\text{O}_2$  combined with sequential Fe (II) catalytic process. *Chemosphere* 180:48–56
- Zheng N, He X, Hu R, Wang R, Zou Q (2022) In-situ production of singlet oxygen by dioxygen activation on iron phosphide for advanced oxidation processes. *Appl Catal B Environ* 307:121157
- Zito P, Podgorski DC, Bartges T (2020) Sunlight-induced molecular progression of oil into oxidized oil soluble species, interfacial material, and dissolved organic matter. *Energy Fuels* 34:4721–4726. <https://doi.org/10.1021/acs.energyfuels.9b04408>

**Publisher's Note** Springer Nature remains neutral with regard to jurisdictional claims in published maps and institutional affiliations.

Springer Nature or its licensor (e.g. a society or other partner) holds exclusive rights to this article under a publishing agreement with the author(s) or other rightsholder(s); author self-archiving of the accepted manuscript version of this article is solely governed by the terms of such publishing agreement and applicable law.